Title

The Association of the Xeroderma Pigmentosum Group D DNA Helicase (XPD) with Transcription Factor IIH Is Regulated by the Cytosolic Iron-Sulfur Cluster Assembly Pathway*

Journal

Journal of Biological Chemistry, 290(22)

ISSN

0021-9258

Authors

Vashisht, Ajay A
Yu, Clarissa C
Sharma, Tanu
et al.

Publication Date

2015-05-01

DOI

10.1074/jbc.m115.650762

Peer reviewed

THE JOURNAL OF BIOLOGICAL CHEMISTRY VOL. 290, NO. 22, pp. 14218–14225, May 29, 2015

The Association of the Xeroderma Pigmentosum Group D DNA Helicase (XPD) with Transcription Factor IIH Is Regulated by the Cytosolic Iron-Sulfur Cluster Assembly Pathway*[S]

Received for publication, March 11, 2015, and in revised form, April 17, 2015 Published, JBC Papers in Press, April 20, 2015, DOI 10.1074/jbc.M115.650762

Ajay A. Vashisht, Clarissa C. Yu, Tanu Sharma, Kevin Ro, and James A. Wohlschlegel[1]

From the Department of Biological Chemistry, David Geffen School of Medicine, University of California, Los Angeles, California 90095

Background: The mechanism by which XPD helicase acquires its Fe-S cluster is unknown.
Results: XPD associates with the CIA targeting complex or TFIIH in two mutually exclusive protein complexes. Blocking Fe-S cluster assembly on XPD inhibits its incorporation into TFIIH.
Conclusion: XPD maturation is a stepwise process in which XPD acquires its Fe-S cluster before binding TFIIH.
Significance: The XPD-CIA targeting complex interaction is required for TFIIH assembly.

Xeroderma pigmentosum group D (XPD) helicase is a component of the transcription factor IIH (TFIIH) transcription complex and plays essential roles in transcription and nucleotide excision repair. Although iron-sulfur (Fe-S) cluster binding by XPD is required for activity, the process mediating Fe-S cluster assembly remains poorly understood. We recently identified a cytoplasmic Fe-S cluster assembly (CIA) targeting complex composed of MMS19, CIAO1, and FAM96B that is required for the biogenesis of extramitochondrial Fe-S proteins including XPD. Here, we use XPD as a prototypical Fe-S protein to further characterize how Fe-S assembly is facilitated by the CIA targeting complex. Multiple lines of evidence indicate that this process occurs in a stepwise fashion in which XPD acquires a Fe-S cluster from the CIA targeting complex before assembling into TFIIH. First, XPD was found to associate in a mutually exclusive fashion with either TFIIH or the CIA targeting complex. Second, disrupting Fe-S cluster assembly on XPD by either 1) depleting cellular iron levels or 2) utilizing XPD mutants defective in either Fe-S cluster or CIA targeting complex binding blocks Fe-S cluster assembly and prevents XPD incorporation into TFIIH. Finally, subcellular fractionation studies indicate that the association of XPD with the CIA targeting complex occurs in the cytoplasm, whereas its association with TFIIH occurs largely in the nucleus where TFIIH functions. Together, these data establish a sequential assembly process for Fe-S assembly on XPD and highlight the existence of quality control mechanisms that prevent the incorporation of immature apoproteins into their cellular complexes.

Xeroderma pigmentosum group D (XPD)[2] helicase, also known as ERCC2 (excision repair cross complementing rodent repair deficiency, complementation group 2), is an essential component of the general transcription factor TFIIH complex and plays critical roles in transcription and nucleotide excision repair (NER). With respect to the NER pathway, XPD possesses a 5′ to 3′ double-stranded DNA helicase activity that is essential for the detection and repair of DNA base damage including pyrimidine dimers and bulky adducts resulting from environmental insults such as UV light and chemical exposure (1). In contrast, the role of XPD in transcription is independent of its helicase activity but requires the structural integrity of the TFIIH complex, which is XPD-dependent. Mutations in XPD have been associated with three clinically distinct autosomal recessive disorders, namely xeroderma pigmentosum, trichothiodystrophy and Cockayne syndrome, highlighting its importance in cellular physiology (2).

A large number of nuclear proteins in recent years including XPD have been shown to bind a Fe-S cluster prosthetic group (3, 4). Fe-S clusters are inorganic cofactors that either function directly in redox reactions or play a structural role in the stabilization of a protein domain (5, 6). The XPD homologue from *Sulfolobus acidocaldarius* was shown to bind a Fe-S cluster that was not required for either its global stability or its single-stranded DNA binding and ATPase activities but was essential for its *in vitro* helicase activity (7). Pugh *et al.* (8) showed that integrity of Fe-S cluster on *Fac*Rad3 (*Ferroplasma acidarmanus*) was necessary for the folding and structural stability of an auxiliary domain required for coupling ATP hydrolysis and translocation activity. X-ray crystallography studies of XPD revealed that the Fe-S cluster was bound to a unique insert embedded within helicase domains 1 and 2 (9–11) and could potentially function by separating duplex DNA at the single-stranded DNA-double-stranded DNA junction. Despite the

* This work was supported, in whole or in part, by National Institutes of Health Grant GM089778 (to J. A. W.). This work was also supported by the University of California Cancer Research Coordinating Committee (to J. A. W.) and the Jonsson Cancer Center at UCLA (to J. A. W.).
[S] This article contains supplemental Table 1.
[1] To whom correspondence should be addressed. Tel.: 310-794-7955; Fax: 310-206-1929; Email: jwohl@mednet.ucla.edu.

[2] The abbreviations used are: XPD, xeroderma pigmentosum group D; NER, nucleotide excision repair; CIA, cytoplasmic iron-sulfur cluster assembly; IP, immunoprecipitation; TFIIH, transcription factor IIH.

importance of the XPD Fe-S cluster in its function, the pathway and the mechanisms by which human XPD acquires its Fe-S cluster are only just beginning to emerge.

The biogenesis of nuclear Fe-S proteins such as XPD is mediated by the cytoplasmic iron-sulfur cluster assembly (CIA) pathway. Recently, our group together with the groups of Roland Lill and Simon Boulton independently identified a novel cytoplasmic protein complex composed of MMS19, CIAO1, and FAM96B that we termed the CIA targeting complex (12, 13). The CIA targeting complex physically associates with a large number of nuclear proteins involved in DNA metabolism including DNA polymerases, nucleases, and helicases (including XPD) as well as other components of the CIA machinery leading to the model that the CIA targeting complex functions as a substrate adapter that recruits apoprotein substrates to the CIA machinery to facilitate Fe-S cluster transfer. Consistent with this model, disruption of the CIA targeting complex step leads to impaired Fe-S cluster assembly for these DNA metabolic proteins (12, 13).

In this report we use XPD as a prototypical nuclear Fe-S protein to further explore the steps involved in Fe-S cluster assembly on XPD. We find that XPD associates with the cytoplasmic CIA targeting complex independently of TFIIH. Inhibiting Fe-S cluster assembly on XPD by either 1) depleting cellular iron levels, 2) mutating the cysteine residues in XPD that participate in Fe-S cluster binding, or 3) mutating the region of XPD required for CIA targeting complex binding blocked the subsequent assembly of XPD into TFIIH. Together, these data suggest that Fe-S cluster assembly occurs in a stepwise manner in which the acquisition of an Fe-S cluster by XPD from the CIA machinery is essential for its incorporation into its cognate cellular complex TFIIH and highlights the presence of a cellular mechanism that ensures Fe-S cluster assembly on XPD is completed before it is allowed to perform its normal cellular functions.

Experimental Procedures

Plasmids—Plasmids containing human XPD (CloneID: LIFESEQ3293238) and mouse p44 (CloneID: 4488798) was purchased from Open Biosystems. Human MMS19 cDNA was a kind gift from Lurdes Queimado (University of Oklahoma). ORFs for XPD, p44, and MMS19 were amplified using primers containing AttB1/2 sites with Phusion TaqDNA polymerase (New England Biolabs) and subcloned into pDONR221 vector using the Gateway cloning system (Invitrogen). XPD-C190S, XPD-R112H, and XPD-Δ277–286 mutants were created by site-directed mutagenesis using overlapping PCR primers harboring the respective mutations. The XPD fragments used to identify the region responsible for binding to MMS19 were constructed by PCR with primers containing AttB sites flanking the region to be amplified, cloned into pDONR221, and subsequently recombined into destination vectors that encode 3×HA-3×FLAG or 6×Myc N-terminal tags as needed using Gateway cloning system.

Cell Culture, Cell Lines, and Plasmid Transfections—All cell lines were cultured in complete Dulbecco's modified Eagle's medium containing 10% fetal bovine serum (Foundation B FBS from Gemini), 100 units/ml penicillin and streptomycin, and 2 mM glutamine at 37 °C in ambient air with 5% CO_2. HEK293, HEK293T, and Flp-In™ T-REx™-293 cells were obtained from the American Type Culture Collection, Thermo Scientific, and Invitrogen, respectively. XPD patient fibroblast line (GM08207) was purchased from Coriell cell repositories. These cells harbor both a R683W mutation and a deletion of amino acids 36–61 in XPD. Flp-In™ T-REx™-293 cell stably expressing 3×HA-3×FLAG-XPD-WT, 3×HA-3×FLAG-XPD-C190S, 3×HA-3×FLAG-XPD-Δ277–286, 3×HA-3×FLAG-mouse p44, and 3×HA-3×FLAG-MMS19 were generated using the Flp-In system (Invitrogen) according to manufacturer's instructions.

Affinity Purification of XPD-WT, XPD-C190S, and Mouse p44 for Identification of Associated Proteins Using MudPIT Analysis—Twelve 15-cm tissue cultures plates of 3×HA-3×FLAG XPD wt, 3×HA-3×FLAG XPD C190S, and 3×HA-3×FLAG p44 expressing Flp-In™ TREx™-293 cells were grown, induced with doxycycline overnight, harvested, and lysed in immunoprecipitation (IP) buffer. Immunoprecipitations were carried out using anti-FLAG-M2 beads followed by elution with FLAG peptide, TCA precipitation, and acetone washes as described previously (12, 14). For proteomic analysis, samples were digested by the sequential addition of Lys-C and trypsin proteases and analyzed by MudPIT (15, 16). A detailed description of the multidimensional peptide fractionation protocol, mass spectrometer settings, and bioinformatic workflow is described in Wohlschlegel (17).

Immunoprecipitation and Immunoblotting—Immunoprecipitation and immunoblotting were performed as described (14). Samples were further analyzed by SDS-PAGE followed by immunoblotting with relevant antibodies.

Antibodies—MMS19 (16015-1-AP) and FAM96B (20108-1-AP) antibodies were purchased from Proteintech Group, Inc. (Chicago, IL). CIAO1 (UCLA852) antibody was generated by Cocalico Biologicals. XPD (sc-101174), XPB (sc-293), cyclin H (sc-609), and c-Myc (sc-789) antibodies were obtained from Santa Cruz Biotechnology Inc. NARFL (SAB 4502760), FLAG-M2 (F1804), and β-tubulin (T5293) antibodies were purchased from Sigma. Horseradish peroxidase-conjugated secondary antibodies were obtained from Jackson ImmunoResearch Laboratories. Immunoprecipitations were carried out using affinity matrices for anti-FLAG M2 (A2220; Sigma).

UV Treatment of XPD Patient Fibroblast, XPD Patient Fibroblast Stably Expressing XPD-WT and XPD-Δ277–286—XPD patient-derived fibroblasts as well as XPD patient fibroblast cells stably expressing XPD-WT or XPD-Δ277–286 were each plated in triplicate. After removing half of the media on the following day, cells were treated with 0 J/M^2, 2 J/M^2, and 3 J/M^2 of UV light (CL-1000 Ultraviolet Crosslinker from UVP, LLC, Upland, CA) with the lid removed. Fresh media was added to the cells after UV treatment, and cells were grown for 7 days before cell viability was measured by cell counting using the TC10 (Bio-Rad) cell counter.

Subcellular Fractionation—Cytosolic and nuclear fractions were prepared from HeLa cells as described (18). The cytosolic and nuclear fractions were suspended in 2× SDS sample buffer, boiled, and analyzed by SDS-PAGE followed by immunoblotting with appropriate antibodies.

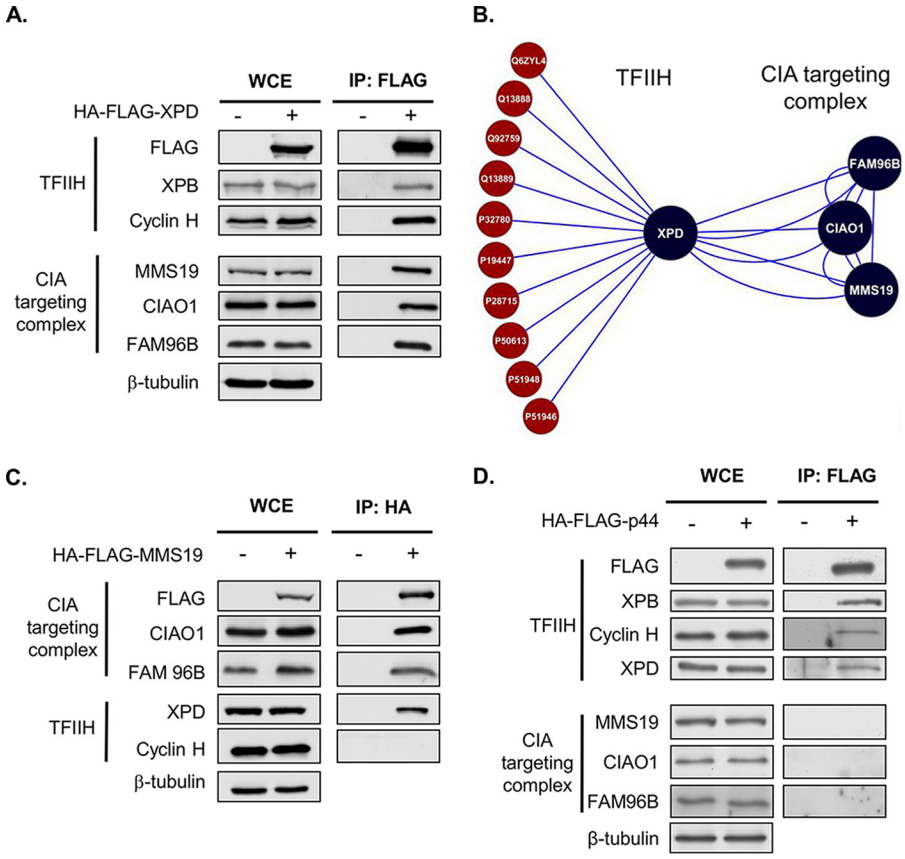

FIGURE 1. **Human XPD associates with TFIIH and the CIA targeting complex in a mutually exclusive manner.** *A*, Flp-In™ TREx™-293-derived stable cells lines expressing HA-FLAG-XPD were induced with doxycycline (500 ng/ml). XPD was immunopurified using FLAG antibodies, and samples were analyzed by SDS-PAGE and blotted with indicated antibodies. *WCE*, whole cell extracts. *B*, schematic summarizing protein interactions identified by proteomic mass spectrometry between XPD, TFIIH components, and the CIA targeting complex. A complete list of the TFIIH and CIA targeting complex components identified in XPD proteomic analysis as well as all identified XPD-interacting proteins can be found in Table 1 and supplemental Table 1, respectively. *C* and *D*, Flp-In™ TREx™-293-derived stable cell lines expressing HA-FLAG-MMS19 (*C*) or HA-FLAG-p44 (*D*) were induced overnight with doxycycline (500 ng/ml), and HA-FLAG-tagged proteins were immunoprecipitated with FLAG antibodies (*HA-FLAG-MMS19* and *HA-FLAG-p44*). Whole cell extracts and immunoprecipitates (*IP*) were immunoblotted with the indicated antibodies. The parental Flp-In™ TREx™-293 cell line was used as a control in all cases.

Results

Identification of XPD-associated Protein Complexes—Although we have previously shown that the assembly of an Fe-S cluster on XPD requires the CIA targeting complex, our understanding for how this interaction is regulated is still very limited. To gain insight into how a prototypical substrate such as XPD associates with the CIA machinery, we conducted a proteomic analysis to identify proteins that co-purify with XPD. Briefly, XPD immunoprecipitates were prepared from HEK293 cells stably expressing HA-FLAG-XPD, digested with trypsin, and then analyzed using proteomic mass spectrometry. As expected, XPD co-purified with known TFIIH subunits (XPB, cyclin H, CDK7, and GTF2H1) as well as the CIA targeting complex (MMS19, CIAO1, and FAM96B) (Fig. 1, *A* and *B*, Table 1). These proteomic results were validated by immunoblotting XPD IPs with CIA targeting complex and TFIIH subunits (Fig. 1*A*). Interestingly, when we compared the XPD proteomic analysis with the proteomic studies of the CIA targeting complex we previously performed, we observed the CIA targeting complex was never found associated with TFIIH subunits other than XPD (Fig. 1*B*). This observation led us to hypothesize that XPD associates with either TFIIH or the CIA targeting complex in two mutually exclusive protein complexes. Instead of a model in which the CIA targeting complex delivers an Fe-S cluster to XPD that is already assembled into TFIIH, this observation suggests that Fe-S cluster assembly more likely occurs in a stepwise manner in which XPD first associates with the CIA targeting complex to acquire its Fe-S cluster and is then subsequently incorporated into TFIIH.

XPD Is Present in Two Mutually Exclusive Protein Complexes—To begin to test this model, we utilized a combination of proteomic mass spectrometry and co-IP experiments to validate XPD mutually exclusive interactions with TFIIH and the CIA targeting complex. First, MMS19 IPs were prepared from HEK293 cells stably expressing HA-FLAG-MMS19 and then analyzed by both immunoblotting and proteomic mass spectrometry. XPD and the CIA targeting complex components (FAM96B and CIAO1) were identified in MMS19 IPs, whereas other TFIIH subunits such as cyclin H were not detectable by either immunoblotting (Fig. 1*C*) or proteomic mass spectrometry (Table 1). Furthermore, TFIIH subunit p44-containing protein complexes isolated from a HEK293 stable cell line contain multiple TFIIH complex subunits including XPB and cyclin H but not members of the CIA targeting complex (Fig.

TABLE 1

Summary of proteomic analysis for XPD-WT-, XPD-C190S-, p44- and MMS19-associated protein complexes

TSC, Peps, and SeqCov refer to total spectral counts, number of different peptides, and percent sequence coverage, respectively, for each identified protein. Numbers shown in bold represents the values for bait protein in each immunoprecipitation. Supplemental Table I contains a complete list of identified proteins in each sample. For detailed information on MMS19 data please refer to previously published proteomic analyses (12).

Complex	Protein (accession no.)	XPD-WT			XPD-C190S			Mouse-p44			MMS19		
		TSC	Peps	SeqCov	TSC	Peps	SeqCov	TSC	Peps	SeqCov	TSC	Peps	SeqCov
CIA targeting complex	MMS19 (Q96T76)	783	93	67.7	475	65	50.1	0	0	0	**6921**	**103**	**64.1**
	CIAO1 (O76071)	441	30	60.8	506	27	60.2	0	0	0	2709	32	58.7
	FAM96B (Q9Y3D0)	115	14	76.7	36	8	44.2	0	0	0	878	29	87.7
TFIIH	ERCC2 (P18074)	**3187**	**101**	**70.9**	**2466**	**72**	**57.6**	156	20	28.9	88	28	34.2
	ERCC3 (P19447)	25	22	26.3	0	0	0	917	45	51.8	0	0	0
	CycH (P51946)	383	41	71.2	9	6	22.3	22	8	33.1	0	0	0
	MAT1 (P51948)	181	39	69.9	4	4	23	33	9	30.4	0	0	0
	CDK7 (P50613)	202	33	41.6	5	4	13.9	37	12	38.2	0	0	0
	GTF2H1 (P32780)	15	9	24.3	0	0	0	112	19	30.3	0	0	0
	GTF2H2C (Q6P1K8)	11	10	26.6	0	0	0	**1006**	**25**	**39.5**	0	0	0
	GTF2H3 (Q13889)	7	4	16.2	0	0	0	87	11	32.8	0	0	0
	GTF2H4 (Q92759)	15	10	28.4	0	0	0	102	10	21.6	0	0	0
	GTF2H5 (Q6ZYL4)	2	2	36.6	0	0	0	31	4	56.3	0	0	0

1*D* and Table 1). These data provide strong evidence that XPD associates with either the CIA targeting complex or TFIIH in mutually exclusive protein complexes and is consistent with a stepwise model for XPD assembly into TFIIH.

XPD Assembly into TFIIH Requires Sufficient Cellular Iron and the Ability to Bind an Fe-S Cluster Cofactor—We reasoned that if Fe-S cluster assembly on XPD is coupled to its incorporation into TFIIH as dictated by our stepwise assembly model, then disrupting Fe-S cluster assembly would block the association of XPD with TFIIH. We tested this possibility using two complementary approaches. First, we examined how TFIIH assembly is affected by changes in cellular iron levels. XPD was immunoprecipitated from cells treated with either ferric ammonium citrate or desferrioxamine mesylate to create iron-rich and iron-deficient conditions, respectively. XPD association with TFIIH subunits XPB and cyclin H was significantly reduced in iron-depleted cells compared with iron-rich cells, whereas association with the CIA targeting complex remained unaltered (Fig. 2*A*). Iron regulatory protein 2 (IRP2), a regulator of iron homeostasis that is stabilized in iron-deficient conditions, was used to assess the efficacy of iron treatment (Fig. 2*A*) (19). Together, these data are consistent with the model in which iron depletion results in impaired Fe-S cluster assembly on XPD leading to its reduced incorporation into TFIIH.

Second, we examined how mutations in XPD that disrupt Fe-S cluster binding affect XPD incorporation into TFIIH. For the archaebacteria *S. acidocaldarius* homologue of XPD, it was shown that mutation of one of the cysteine residues predicted to coordinate Fe-S cluster binding leads to loss of Fe-S cluster assembly as well as XPD DNA helicase activity (7). We characterized the analogous C190S mutant in human XPD for its ability to assemble into functional TFIIH complexes. A proteomic analysis as well as co-IP assays performed from HEK293 cells expressing the XPD-C190S mutant revealed that the mutant retained the ability to bind the CIA targeting complex but failed to interact with the TFIIH subunits XPB and cyclin H (Table 1, Fig. 2*B*, supplemental Table 1), suggesting that Fe-S cluster binding by XPD is required for its incorporation into TFIIH. These results are consistent with genetic studies in *Saccharomyces cerevisiae* in which a strain expressing the analogous XPD cysteine mutant displays increased UV sensitivity and defects in the repair of photo adducts by the NER pathway, phenotypes that are consistent with impaired TFIIH function (7).

In addition to XPD C190S, we also examined the effects of the XPD mutation R112H on its ability to assemble into functional TFIIH complexes (2). The R112H mutation is associated with the clinical disorder trichothiodystrophy and was previously shown to disrupt XPD's Fe-S cluster binding properties, presumably due to its proximity to one of XPD's Fe-S cluster-coordinating cysteine residues (7). This mutation has also been shown to result in the loss of helicase activity *in vitro* and defective NER *in vivo* (20). In Fig. 2*C* we find that the R112H mutant fails to associate with TFIIH while retaining the ability to bind to the CIA targeting complex (Fig. 2*C*). Together, these data further strengthen the argument that the proper assembly of XPD's Fe-S cluster is an essential prerequisite for its incorporation into and the proper functioning of TFIIH.

The Physical Association of XPD with MMS19 Is Required for Both Its Incorporation into TFIIH and DNA Repair—Elucidating how the CIA targeting complex recognizes substrates such as XPD is critical for understanding the Fe-S cluster assembly process. To begin to address this question, we sought to identify the region of XPD that mediates its association with the CIA targeting complex and then assess the functional consequences of disrupting this binding interface. To identify the interacting domain, we generated an extensive collection of XPD fragments lacking different regions of the protein and assessed their ability to co-immunoprecipitate with MMS19 in a transient transfection assay (data are summarized in Fig. 3*A*). We observed that a fragment of XPD spanning amino acids 276–761 was capable of binding to MMS19, whereas a fragment containing amino acids 286–761 lost this ability. These data suggest that the region of XPD responsible for MMS19 binding lies between amino acids 276 and 286. To validate this finding, we constructed a full-length XPD mutant specifically lacking this region (Δ277–286) and confirmed that this mutant lost the ability to interact with MMS19 (Fig. 3*B*). Consistent with our stepwise assembly model, the XPD-Δ277–286 also lost the ability to bind to TFIIH (Fig. 3*B*). We also utilized this mutant to examine the functional relevance of the XPD-MMS19 interaction with respect to DNA repair. It has previously been shown

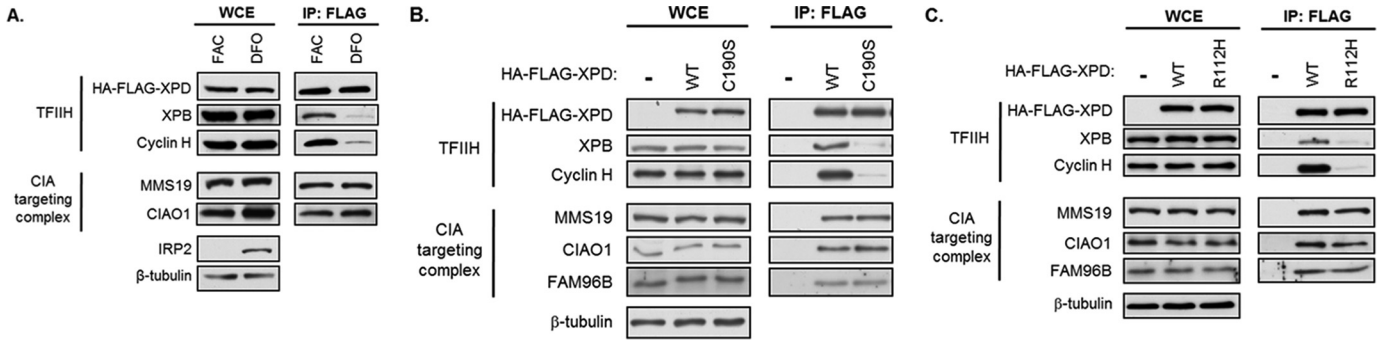

FIGURE 2. **Incorporation of XPD into TFIIH requires both adequate cellular iron levels and the ability of XPD to coordinate an Fe-S cluster.** *A*, Flp-In™ TREx™-293 cells stably expressing 3HA-3FLAG-XPD or control cells were induced overnight with doxycycline (500 ng/ml) and treated for 8 h with 100 μg/ml ferric ammonium citrate (*FAC*; Thermo Fisher Scientific) or 100 μM desferrioxamine mesylate (*DFO*; Sigma). HA-FLAG-XPD was immunoprecipitated with FLAG antibody. Whole cell extract (*WCE*) and immunoprecipitates (*IP*) were probed with the indicated antibodies. *B* and *C*, Flp-In™ TREx™-293 derived cell lines stably expressing HA-FLAG-XPD-WT, HA-FLAG-XPD-C190S, or HA-FLAG-XPD-R112H were induced overnight with doxycycline (500 ng/ml). Cell lysates were prepared, and HA-FLAG-XPD wild type and mutant proteins were immunoprecipitated using FLAG antibody. WCE and immunoprecipitates were blotted with indicated antibodies.

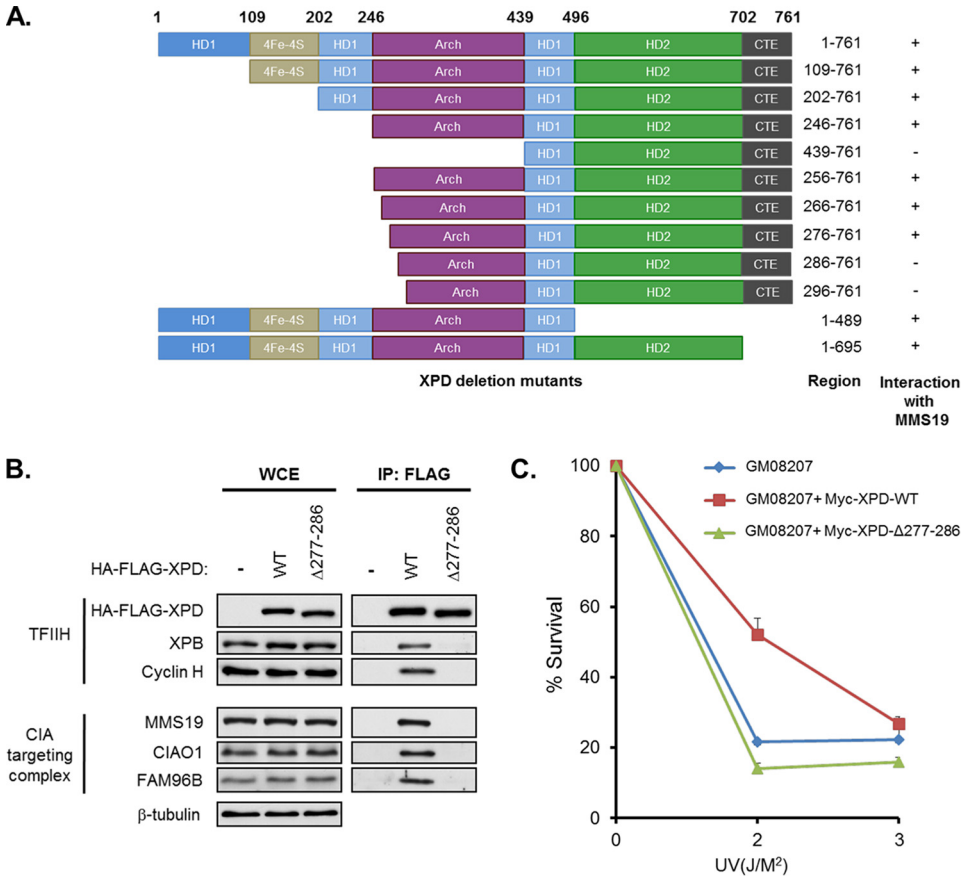

FIGURE 3. **XPD associates with MMS19 via a peptide docking site that is indispensable for its assembly into TFIIH and its DNA repair functions.** *A*, summary of protein-protein interaction studies performed using co-immunoprecipitation assays between a series of XPD deletion mutants and MMS19. *B*, Flp-In™ TREx™-293 cells stably expressing HA-FLAG-XPD-WT, HA-FLAG-XPD-Δ277–286, or control cells were induced overnight with doxycycline (500 ng/ml). Whole cell extracts (*WCE*) and immunoprecipitates (*IP*) using FLAG antibody were probed with the indicated antibodies. *C*, XPD patient fibroblast cells (GM08207) were obtained from Coriell Institute for Medical Research and complemented with XPD-WT and XPD-Δ277–286 (defective in MMS19 binding) and were tested for their sensitivity to UV irradiation. The number of viable cells was counted for each set after 7 days of UV treatment, and % survival rate was plotted as mean ± S.E. ($n = 3$).

that fibroblasts derived from xeroderma pigmentosum patients harboring mutations in XPD display increased sensitivity to UV-induced DNA damage due to defects in the NER pathway (21) and this mutant phenotype can be rescued by expression of wild type XPD (22). Utilizing this experimental system, we tested whether the XPD-Δ277–286 mutant that is defective in MMS19 binding is able to complement the UV sensitivity phenotype of XPD-deficient fibroblasts. We find that although the expression of wild type XPD was able to rescue the UV sensitivity defects seen in these cells, the expression of the XPD-Δ277–286 mutant did not rescue the phenotype, suggesting that this mutant was incapable of fully supporting NER (Fig.

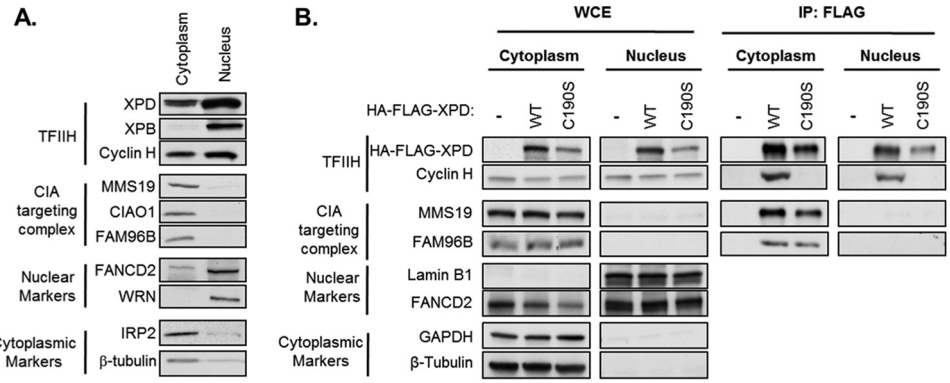

FIGURE 4. **Subcellular distribution of XPD, TFIIH, and the CIA targeting complex.** *A*, nuclear and cytoplasmic fractions were prepared from HeLa cells and immunoblotted with antibodies against TFIIH components (XPD, XPB, and cyclin H), CIA targeting complex proteins (MMS19, CIAO1, and FAM96B), and nuclear (*WRN*) and cytosolic (iron regulatory protein 2 (*IRP2*) markers. *B*, HA-FLAG-XPD-WT was immunoprecipitated using FLAG beads from nuclear and cytoplasmic fractions prepared from Flp-In™ TREx™-HeLa cells stably expressing HA-FLAG-XPD-WT after overnight induction with doxycycline (500 ng/ml). WCE and immunoprecipitates (*IP*) were blotted with the indicated antibodies.

3*C*). The results further highlight the functional importance of the MMS19-XPD interaction in mediating Fe-S cluster assembly of XPD and its subsequent incorporation into active TFIIH. These data also identify a docking site in XPD that is required for recognition by the CIA targeting complex, which may have important implications for recognition of Fe-S proteins by the CIA targeting complex (see "Discussion").

Subcellular Localization of the CIA Targeting Complex and XPD—Although large numbers of Fe-S proteins reside in the both the cytoplasm and nucleus, it is unknown where Fe-S assembly typically takes places for these proteins. Does Fe-S cluster assembly for a given protein occur in the compartment in which it functions (*i.e.* in the nucleus for XPD), or does Fe-S cluster assembly occur at defined sites irrespective of the final destination of the protein? To address this question for XPD, we examined whether its association with the CIA targeting complex occurs in the cytoplasm or nucleus using a subcellular fractionation approach. Cytosolic and nuclear fractions were prepared from HeLa cells by hypotonic lysis and analyzed by immunoblotting for endogenous TFIIH and CIA targeting complex components (Fig. 4*A*). We find that the CIA targeting complex is present almost exclusively in the cytoplasmic fraction, whereas XPD is distributed between both cytoplasmic and nuclear fractions. TFIIH components XPB and cyclin H are both enriched in the nuclear fraction, consistent with their essential functions in nuclear processes, although a pool of cytoplasmic cyclin H is also detectable. The presence of both XPD and the CIA targeting complex in the cytoplasm and the absence of the CIA targeting complex in the nucleus suggest that Fe-S assembly on XPD is likely a cytoplasmic event. Second, we performed co-IP experiments in HeLa cells stably expressing HA-FLAG-XPD and showed that both wild type XPD and the XPD-C190S mutant associate with the CIA targeting complex (MMS19 and FAM96B) in the cytosolic fraction (Fig. 4*B*). Wild type XPD associates with the TFIIH subunit cyclin H in both nuclear and cytoplasmic fractions, whereas XPD-C190S fails to assemble into TFIIH as expected (Fig. 4*B*). Together, these results are consistent with a stepwise assembly model for XPD in which XPD first associates with the CIA targeting complex subunit in the cytoplasm to acquire its Fe-S cluster, after which it is incorporated into TFIIH to perform its essential functions in transcription and NER. It is worth noting, however, that these data do not provide significant insight into where TFIIH is itself assembled, as XPD could either 1) associate with TFIIH in the cytoplasm and then translocate to the nucleus or 2) TFIIH and XPD could be independently imported into the nucleus and assemble into a functional TFIIH complex there.

Discussion

Our data support a model in which the maturation of the Fe-S enzyme XPD occurs in a stepwise process where 1) apoXPD is recruited to the CIA machinery via interactions with the CIA targeting complex, 2) XPD acquires its Fe-S cluster, and 3) Fe-S cluster-bound XPD is released from the CIA machinery, enabling it to assemble into the TFIIH complex. We present two major pieces of evidence to substantiate this model (Fig. 5). First, we demonstrate that XPD is associated with either the CIA targeting complex or TFIIH in two mutually exclusive complexes. This observation suggests that the substrate of the CIA targeting complex is free XPD and not TFIIH-associated XPD and that the metallation of XPD and XPD's assembly into TFIIH are temporally distinct events. Second, we clearly establish that blocking Fe-S cluster assembly on XPD using a combination of mutational and pharmacological approaches also inhibits its assembly into TFIIH, suggesting that Fe-S cluster assembly on XPD is required for its subsequent incorporation into TFIIH and proper TFIIH function. Together, these data provide a framework for understanding the pathway mediating the CIA targeting complex-dependent Fe-S cluster assembly on XPD (Fig. 5). Considering XPD is one of dozens of Fe-S proteins that associate with the CIA targeting complex and require its activity for their maturation, this stepwise assembly pathway may ultimately be generalizable to many other extramitochondrial Fe-S proteins.

The molecular basis underlying this stepwise assembly process is unclear, but we envision at least two potential mechanisms by which assembly of XPD into TFIIH could be inhibited until Fe-S cluster assembly on XPD is complete. First, Fe-S cluster binding by XPD could stabilize a protein-protein interaction domain that mediates its binding TFIIH. In the absence of an Fe-S cluster, this domain is incapable of recognizing and/or

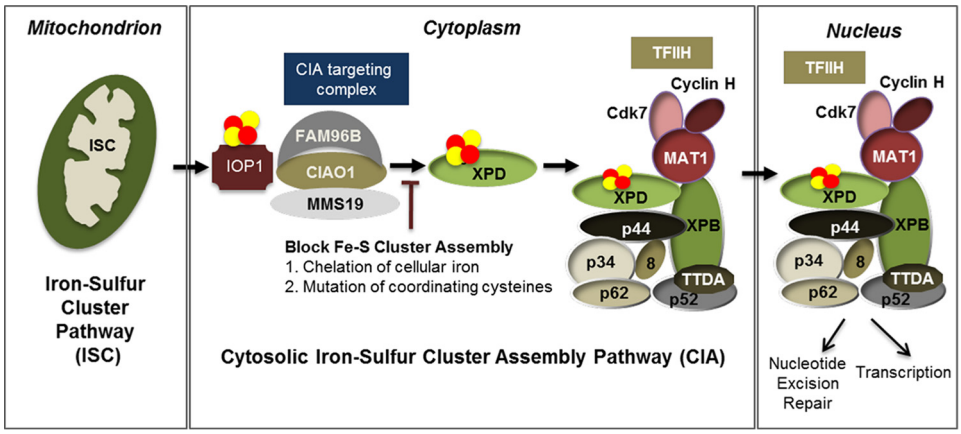

FIGURE 5. **Fe-S cluster assembly of XPD is required for its integration into TFIIH.** Extramitochondrial Fe-S cluster biogenesis depends on the activity of the mitochondrially localized iron-sulfur cluster (*ISC*) biogenesis machinery, which generates an as of yet unidentified sulfur-based compound that is exported to the cytosol (5). The cytoplasmic iron-sulfur cluster assembly (CIA pathway) then catalyzes the assembly of Fe-S clusters on cytoplasmic protein scaffolds, which are subsequently transferred to apoproteins in a manner dependent on the iron-only hydrogenase IOP1 and the CIA targeting complex (MMS19, CIAO1, and FAM96B) (12). Our data suggest that Fe-S cluster delivery to apoproteins such as XPD occurs in the cytoplasm via a stepwise pathway in which XPD is first recruited to the CIA machinery via direct protein-protein interactions. XPD then remains stably associated with the CIA targeting complex until cluster transfer is completed, which then triggers its release and subsequent assembly into TFIIH. Once TFIIH is properly assembled, it translocates into the nucleus where it performs its essential functions in transcription and DNA repair. Inhibiting Fe-S cluster assembly during this process results in the sequestration of XPD by the CIA targeting complex preventing the incorporation of apoXPD into TFIIH.

binding to TFIIH. Alternatively, the metallation status of XPD may regulate its association with the CIA targeting complex. In this scenario, the CIA targeting complex would recognize and bind specifically to apoXPD and sequester it away from TFIIH. Insertion of an Fe-S cluster into XPD would then trigger its release from the CIA targeting complex and enable it to assemble into TFIIH complexes. This mechanism would act essentially as an Fe-S cluster assembly checkpoint that would ensure that the maturation of an Fe-S protein is completed before it is allowed to assemble into its normal cognate cellular complex.

In this work we identified a region in XPD spanning amino acids 277–286 that is essential for its interaction with MMS19 (Fig. 3). Surprisingly, this peptide sequence resides in a loop in the arch domain of XPD that is distinct from the Fe-S domain (9–11). These data suggest that substrate recognition of XPD by the CIA targeting complex likely occurs in a bipartite manner in which the CIA targeting complex is first recruited to XPD via a distal docking sequence that then facilitates the insertion of an Fe-S cluster into the Fe-S cluster binding domain of XPD. Apoprotein recognition in this manner is reminiscent of the recognition of LYR motifs in mitochondrial Fe-S recipients by the co-chaperone HSC20 and may suggest a general paradigm for Fe-S protein recognition (23). However, the extent to which docking sequence-dependent recognition of apoXPD by the CIA targeting complex can be generalized to other Fe-S proteins remains unclear. Considering that the MMS19 docking site we identified in XPD during this does not appear to be strongly conserved at the primary sequence level in other CIA targeting complex-associated Fe-S proteins, there may be other as of yet undiscovered mechanisms that govern substrate recognition in this pathway.

Eukaryotic Fe-S protein biogenesis is a highly compartmentalized process with discrete steps occurring in both the mitochondria and the cytoplasm. (Fig. 5). It has been unclear, however, the extent to which the maturation of extramitochondrial Fe-S proteins is spatially regulated. For example, it is unknown whether nuclear Fe-S proteins acquire their Fe-S clusters from the CIA machinery in the cytoplasm before their nuclear import or in the nucleus after their translocation. Moreover, the presence of Fe-S cluster assembly machinery in both the cytoplasm and nucleus has done little to clarify this issue. Our results indicate that the interaction of XPD with the CIA targeting complex occurs primarily in the cytoplasm, whereas its interaction with TFIIH is predominantly nuclear (Fig. 4*B*). Although not definitive, these observations are consistent with the CIA targeting complex-dependent transfer of an Fe-S cluster to XPD occurring in the cytoplasm before its assembly into TFIIH and nuclear translocation. This type of spatial regulation may be critically important in the context of the "Fe-S cluster assembly checkpoint" described earlier, which might exist to ensure that the maturation of XPD is performed in a permissive cytoplasmic microenvironment and must be completed before mature, fully functional XPD is allowed to associate with TFIIH. It should be noted that we do not know at this time whether this aspect of XPD maturation can be generalized to other nuclear Fe-S Proteins. It is also not known whether Fe-S cluster assembly and/or repair on XPD can occur in the nucleus under specialized circumstances.

References

1. Friedberg, E. C. (2001) How nucleotide excision repair protects against cancer. *Nat. Rev. Cancer* **1,** 22–33
2. Lehmann, A. R. (2001) The xeroderma pigmentosum group D (XPD) gene: one gene, two functions, three diseases. *Genes Dev.* **15,** 15–23
3. Netz, D. J., Mascarenhas, J., Stehling, O., Pierik, A. J., and Lill, R. (2014) Maturation of cytosolic and nuclear iron-sulfur proteins. *Trends Cell Biol.* **24,** 303–312
4. Ye, H., and Rouault, T. A. (2010) Human iron-sulfur cluster assembly, cellular iron homeostasis, and disease. *Biochemistry* **49,** 4945–4956
5. Lill, R. (2009) Function and biogenesis of iron-sulphur proteins. *Nature* **460,** 831–838
6. Ye, H., and Rouault, T. A. (2010) Erythropoiesis and iron sulfur cluster biogenesis. *Adv. Hematol.* **2010,** 329394
7. Rudolf, J., Makrantoni, V., Ingledew, W. J., Stark, M. J., and White, M. F.

(2006) The DNA repair helicases XPD and FancJ have essential iron-sulfur domains. *Mol. Cell* **23,** 801–808
8. Pugh, R. A., Honda, M., Leesley, H., Thomas, A., Lin, Y., Nilges, M. J., Cann, I. K., and Spies, M. (2008) The iron-containing domain is essential in Rad3 helicases for coupling of ATP hydrolysis to DNA translocation and for targeting the helicase to the single-stranded DNA-double-stranded DNA junction. *J. Biol. Chem.* **283,** 1732–1743
9. Fan, L., Fuss, J. O., Cheng, Q. J., Arvai, A. S., Hammel, M., Roberts, V. A., Cooper, P. K., and Tainer, J. A. (2008) XPD helicase structures and activities: insights into the cancer and aging phenotypes from XPD mutations. *Cell* **133,** 789–800
10. Wolski, S. C., Kuper, J., Hänzelmann, P., Truglio, J. J., Croteau, D. L., Van Houten, B., and Kisker, C. (2008) Crystal structure of the FeS cluster-containing nucleotide excision repair helicase XPD. *PLoS Biol.* **6,** e149
11. Liu, H., Rudolf, J., Johnson, K. A., McMahon, S. A., Oke, M., Carter, L., McRobbie, A. M., Brown, S. E., Naismith, J. H., and White, M. F. (2008) Structure of the DNA repair helicase XPD. *Cell* **133,** 801–812
12. Stehling, O., Vashisht, A. A., Mascarenhas, J., Jonsson, Z. O., Sharma, T., Netz, D. J., Pierik, A. J., Wohlschlegel, J. A., and Lill, R. (2012) MMS19 assembles iron-sulfur proteins required for DNA metabolism and genomic integrity. *Science* **337,** 195–199
13. Gari, K., León Ortiz, A. M., Borel, V., Flynn, H., Skehel, J. M., and Boulton, S. J. (2012) MMS19 links cytoplasmic iron-sulfur cluster assembly to DNA metabolism. *Science* **337,** 243–245
14. Vashisht, A. A., Zumbrennen, K. B., Huang, X., Powers, D. N., Durazo, A., Sun, D., Bhaskaran, N., Persson, A., Uhlen, M., Sangfelt, O., Spruck, C., Leibold, E. A., and Wohlschlegel, J. A. (2009) Control of iron homeostasis by an iron-regulated ubiquitin ligase. *Science* **326,** 718–721
15. Washburn, M. P., Wolters, D., and Yates, J. R., 3rd. (2001) Large-scale analysis of the yeast proteome by multidimensional protein identification technology. *Nat. Biotechnol.* **19,** 242–247
16. Wolters, D. A., Washburn, M. P., and Yates, J. R., 3rd. (2001) An automated multidimensional protein identification technology for shotgun proteomics. *Anal. Chem.* **73,** 5683–5690
17. Wohlschlegel, J. A. (2009) Identification of SUMO-conjugated proteins and their SUMO attachment sites using proteomic mass spectrometry. *Methods Mol. Biol.* **497,** 33–49
18. Lam, Y. W., and Lamond, A. I. (2006) *Isolation of Nucleoli in Cell Biology: A Laboratory Handbook*, pp. 103–107, Elsevier, Burlington, MA
19. Guo, B., Brown, F. M., Phillips, J. D., Yu, Y., and Leibold, E. A. (1995) Characterization and expression of iron regulatory protein 2 (IRP2). Presence of multiple IRP2 transcripts regulated by intracellular iron levels. *J. Biol. Chem.* **270,** 16529–16535
20. Dubaele, S., Proietti De Santis, L., Bienstock, R. J., Keriel, A., Stefanini, M., Van Houten, B., and Egly, J. M. (2003) Basal transcription defect discriminates between xeroderma pigmentosum and trichothiodystrophy in XPD patients. *Mol. Cell* **11,** 1635–1646
21. Protić-Sabljić, M., and Kraemer, K. H. (1986) Reduced repair of non-dimer photoproducts in a gene transfected into xeroderma pigmentosum cells. *Photochem. Photobiol.* **43,** 509–513
22. Gözükara, E. M., Parris, C. N., Weber, C. A., Salazar, E. P., Seidman, M. M., Watkins, J. F., Prakash, L., and Kraemer, K. H. (1994) The human DNA repair gene, ERCC2 (XPD), corrects ultraviolet hypersensitivity and ultraviolet hypermutability of a shuttle vector replicated in xeroderma pigmentosum group D cells. *Cancer Res.* **54,** 3837–3844
23. Maio, N., Singh, A., Uhrigshardt, H., Saxena, N., Tong, W. H., and Rouault, T. A. (2014) Cochaperone binding to LYR motifs confers specificity of iron sulfur cluster delivery. *Cell Metab.* **19,** 445–457